CrossMark

Composition Dependences of Entropy Change and Transformation Temperatures in Ni-rich Ti–Ni System

K. Niitsu[1,2] · Y. Kimura[1] · X. Xu[1] · R. Kainuma[1]

Abstract For Ni-rich Ti–Ni alloys, physical properties such as specific heat and electric resistance were systematically investigated. The B2/B19′ martensitic transformation temperatures ranging from 180 to 373 K were determined for Ni contents of 49.98–51.09 %, and a sudden disappearance of martensitic transformation was confirmed for Ni contents greater than 51.23 %, which has also been well reported in the literatures. The entropy change was also evaluated from differential scanning calorimeter measurement, and it was clarified that the entropy change plotted to T_0 temperature shows an S-shaped curve, starting to drastically decrease at about 300 K. Thermodynamic approaches were then carried out attempting to determine the reason for the disappearance of transformation. The entropy change estimated from direct measurements of specific heats for 51.75 Ni (B2) and 50.92 Ni (B19′) was found to be more consistent with the experimental data, rather than the calculated curve based on the Debye model for vibration specific heat. It was proposed that the equilibrium between the parent and martensite phases obeys the Clausius–Clapeyron relationship in the composition–temperature system. Using the constructed composition–temperature diagram, the disappearance of martensitic transformation in the Ti–Ni system can be well understood as being due to the drastic increase of hysteresis at low temperature.

Introduction

Ti–Ni shape memory alloy (SMA) is the most studied and technologically important SMA system possessing excellent shape memory and superelastic properties. By virtue of some of its practical advantages such as good mechanical properties and corrosion resistance, technological refinements in the fabrication of Ti–Ni SMA have been well established and indeed it has been widely used for various industrial and medical applications. Meanwhile, from the scientific viewpoint, Ti–Ni and its derived SMA systems continue to engender fundamental interest in the nature of B2/B19′ martensitic transformation (MT). In the Ni-rich portion of the Ti–Ni system, it is well known that the MT start temperature (T_{Ms}) suddenly disappears at around 51.4 at.% Ni [1]. Such a suppression of MT has only been explained so far by the concept of strain glass, which is one of the class of glassy states in transformation strain essentially similar to spin glass and relaxor [2, 3]. This concept explains the anomaly observed in the parent (P) state of high-Ni content alloys on the basis of the breaking of strain order. However, no consensus has been

✉ R. Kainuma
  kainuma@material.tohoku.ac.jp

  K. Niitsu
  koudai.niitsu@riken.jp

  Y. Kimura
  yuta.kimura.s8@dc.tohoku.ac.jp

  X. Xu
  xu@material.tohoku.ac.jp

1 Department of Materials Science, Graduate School of Engineering, Tohoku University, Sendai 980-8579, Japan

2 Center for Emergent Matter Science, RIKEN, Wako 351-0198, Japan

reached and the origin of the disappearance of MT is still under discussion.

Very recently, our group has reported superelastic behavior in the temperature region down to 40 K in a Ti–51.8Ni alloy, whose composition is in the strain glass region exhibiting no thermally induced MT [4]. This study revealed that the entropy change, ΔS, estimated by the Clausius–Clapeyron (CC) equation from critical stresses of stress-induced transformation (SIT), σ_{Ms} (forward SIT start stress) and σ_{Af} (reverse SIT finish stress), obtained at many different temperatures, shows a decrement curve toward zero with decreasing temperature and that the superelastic stress hysteresis, σ_{hys}, defined by $\sigma_{Ms}-\sigma_{Af}$, dramatically increases with decreasing temperature. These findings imply that the individual considerations of temperature dependences of the equilibrium SIT stress, σ_0 ($\approx(\sigma_{Ms} + \sigma_{Af})/2$) [5] and σ_{hys} within the frameworks of thermodynamics and kinetics of MT, respectively, are mandatory, especially in the low-temperature region.

In the present study, characteristic temperatures (T_{Ms}, the reverse MT finish temperature, T_{Af}, and equilibrium MT temperature, T_0) and specific heat of Ni-rich Ti–Ni alloys were precisely determined and the MT behavior was studied. Especially, clarification of the origin of the disappearance of MT was attempted by consideration of transformation entropy change, ΔS.

Experimental Procedures

$Ti_{100-x}Ni_x$ alloy ingots, listed in Table 1, were prepared by arc melting under an argon atmosphere. The obtained buttons were homogenized at 1173 K for 30 h in a vacuum followed by water quenching. In order to confirm whether they exhibit the thermally induced MT or not, thermal analysis and electrical resistivity (ER) measurement were performed using a differential scanning calorimeter (DSC) and the physical property measurement system (PPMS),

respectively. Temperature sweeping rates for these measurements were set to ±5 K/min. Latent heat of MT was measured by a high-resolution DSC (Netzsch DSC 204 F1 Phoenix) with a heating rate of 10 K/min. Isobaric specific heat (c_P) was measured by the relaxation method in the temperature region below 300 K using PPMS. The chemical compositions of samples were checked by an electron probe microanalyzer (EPMA) and determined as listed in Table 1, where the error bar is in about ±0.1 at.% Ni. In this paper, prepared alloys are represented with their analytical compositions (e.g., 49.98 Ni) or mole fractions (e.g., $x = 0.4998$).

Results and Discussion

Determination of Transformation Temperatures

The results of DSC measurements for the 49.98, 50.55, and 50.92 Ni alloys are presented in Fig. 1a. They all show clear exothermal and endothermal peaks accompanied by the forward and reverse MTs, onset and offset temperatures being defined as T_{Ms} and T_{Af} (open and filled triangles), respectively.

ER vs temperature curves are presented in Fig. 1b, in which the ER values are normalized by that at 350 K. In 50.55, 50.71, 50.92, and 51.09 Ni specimens, the MT is obviously detected as a drastic change of ER and thermal hystereses associated with the MT are confirmed, T_{Ms} and T_{Af} being indicated by open and filled triangles, respectively. It should also be noted that although the ER curves have a positive temperature dependency in the martensite (M) phase, they hardly show temperature dependence in the P phase. Such ER flow has already been observed in the system exhibiting the B2–B19′ MT [6, 7].

In contrast, the ER curves of 51.23, 51.54, and 51.75 specimens show no apparent change due to MT, whereas

Table 1 Analytical compositions, characteristic temperatures, latent heat, and entropy change of the prepared alloys

Ni content (at.%)		T_{Ms} (K) in ER	T_{Af} (K) in ER	T_0 (K) in ER	T_{Ms} (K) in DSC	T_{Af} (K) in DSC	T_0 (K) in DSC	T_p (K) in DSC[a]	Q^{M-P} (J/mol)[a]	ΔS (J/mol K)
Nominal	Analytical									
50.00	49.98				338	373	355.5	363.1	1641	4.52
50.50	50.55	282	311	296.5	285	320	302.5	307.6	1344	4.37
50.75	50.71	264	288	276				289.5	1223	4.22
51.00	50.92	225	250	237.5	218	250	234	226.2	530	2.34
51.20	51.09	180	216	198						
51.40	51.23	n.d.	n.d.	n.d.						
51.60	51.54									
51.80	51.75									

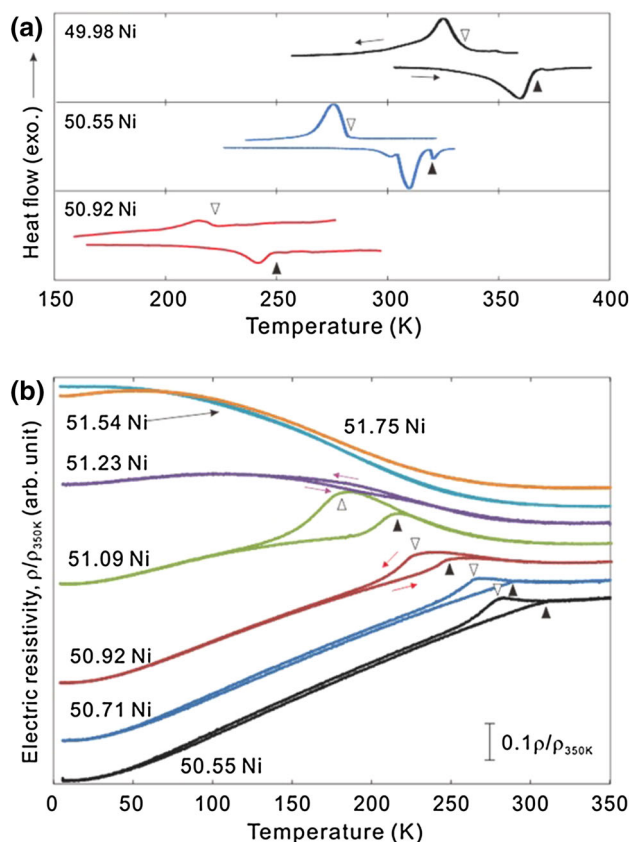[a] T_p and Q^{M-P} are determined using high-resolution DSC

Fig. 1 **a** DSC curves for 49.98, 50.55, and 50.92 Ni specimens. **b** ER vs temperature curves for 50.55, 50.71, 50.92, 51.09, 51.23, 51.54, and 51.75 Ni specimens

Fig. 2 Critical temperatures, T_0, T_{Ms}, and T_{Af}, as a function of Ni content [1, 7, 10–17]

that of the 51.23 sample has a faint hysteresis at around 180 K. Although the origin of this small hysteresis is not clear, no MT could be detected by other techniques. These results suggest that these three specimens kept the P phase condition down to 4 K. It is seen that the ER curves started to increase at around 300 K with decreasing temperature, becoming almost constant in the temperature region below ∼100 K. Such a negative temperature dependence of the ER curve has been reported in some previous papers on not only Ni-rich Ti–Ni alloys, but also Ti–Ni–Fe (more than 6 at.% Fe) alloys [6, 8, 9], which is discussed in relation to the concept of strain glass by Ren et al. [3].

All the determined characteristic temperatures, T_0, T_{Ms}, and T_{Af}, are listed in Table 1 and plotted in Fig. 2 as a function of x together with data from some previous reports [1, 7, 10–17], T_0 being approximated as the average of T_{Ms} and T_{Af} in this study. T_{Ms} in 49.98 Ni (338 K) well accords with that in the slowly cooled stoichiometric TiNi (333 K) [16]. As x increases, T_0, T_{Ms}, and T_{Af} tend to decrease linearly with maintaining an almost constant T_{hys}, and a deviation from this linearity starts to be visible at 50.92 Ni. In $x > 51.09$, T_{Ms} and T_{Af} are not detected down to ∼0 K;
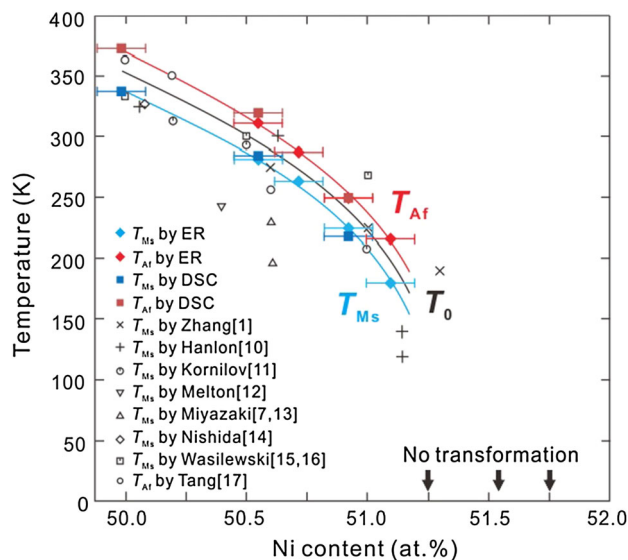
disappearance of MT actually occurs between 51.09 and 51.23 Ni.

Transformation Entropy Change

$\Delta S_{exp}\left(= S_{exp}^{P} - S_{exp}^{M}\right)$ was evaluated as $\Delta S_{exp} = Q^{M \to P}/T_p$ from latent heat, $Q^{M \to P}$, and peak temperature, T_p, in the reverse MT determined by high-resolution DSC. All the numerical data obtained by DSC examinations are listed in Table 1 and plotted as a function of T_0 in Fig. 3, together with some data reported in Ref. [18–20]. In addition to them, some data evaluated by a different method are also plotted with red filled squares in this figure. In this method, ΔS_{exp} was estimated from temperature dependence of σ_0 in
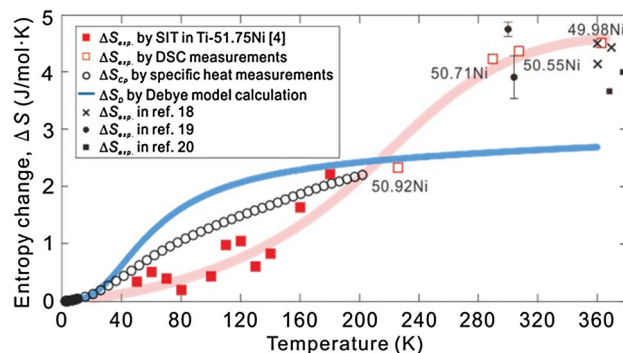

Fig. 3 Entropy changes, ΔS_{exp}, ΔS_{CP}, and ΔS_D, obtained from experiments [4, 18–20], specific heat measurement, and Debye model calculation, respectively, as a function of temperature

the superelastic 51.8 Ni specimen via the following CC equation in the σ_0–T coordinate [4]:

$$\frac{d\sigma_0}{dT} = -\frac{\Delta S}{\varepsilon \cdot V_m}. \tag{1}$$

with the ideal full transformation strain ε and the molar volume V_m. The 51.8 Ni alloy used in that paper is the same as that in the present study, and the analyzed composition is 51.75 Ni. It should be noted that the present data plotted in Fig. 3 are almost 2/3 of those reported in Ref. [4], because in this study ΔS_{exp} was re-estimated using a more relevant value of ε (=0.044), but not an incorrect value of 0.06 used in the literature, in conversion by Eq. 1, where the relevant value of ε in compressive stress was obtained by the Taylor model for a polycrystalline specimen with no texture [21]. As shown in Fig. 3, the present data are very consistent with all other data, and the fitting curve shows an S-shape.

Specific Heat Measurements

In order to examine the temperature dependence of ΔS especially at low temperatures, specific heat measurements were carried out by PPMS. Figure 4 shows resultant c_P in a c_P/T–T^2 coordinate. As shown in this figure, almost complete linearity is confirmed for data obtained at temperatures lower than ~ 7 K ($T^2 < 50$) for all the specimens. As a general approach, the relationship between c_P and temperature (T) can be expressed as

$$\frac{c_P}{T} \approx \beta T^2 + \gamma, \tag{2}$$

where γ is the electronic specific heat coefficient [22]. The coefficient β can be used to obtain the apparent Debye temperature, Θ_D, as
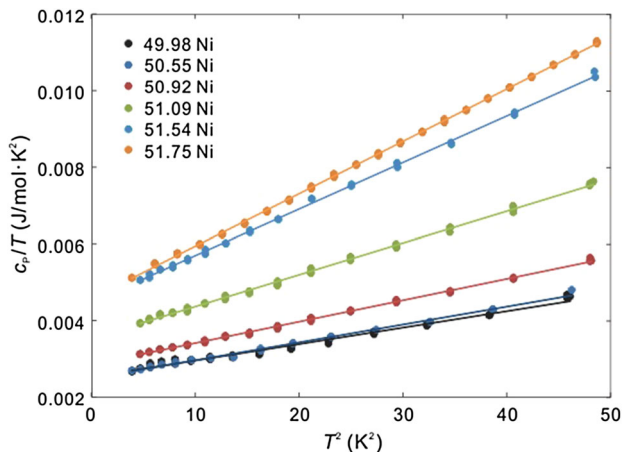
Fig. 4 Temperature dependences of isobaric specific heat, c_P, in a c_P/T–T^2 coordinate determined for M (49.98, 50.55, 50.92, and 51.09 Ni) and P (51.54 and 51.75 Ni) phases

$$\Theta_D \approx \left(\frac{12\pi^4 R}{5\beta}\right)^{1/3}, \tag{3}$$

where R is the gas constant [22]. The values of Θ_D and γ derived from Eqs. 2–3 are listed in Table 2 and plotted as a function of Ni content in Fig. 5a, b together with reference data [6]. First, an anomalously small Θ_D in the P phase is observed, thought to be the result of inherent lattice instability, which is referred to as the resultant of the softening of a TA$_2$[110] phonon branch at the position $q \sim 1/3[110]2\pi/a$ [23–25]. Qualitatively, a larger γ suggests a larger electronic density of states (DOS) at the Fermi energy level ($D(\varepsilon_F)$). The smaller $D(\varepsilon_F)$ in the M phase than in the P phase in $x \leq 51.09$ seems to be consistent with the Kakeshita's reports [6, 26], where $D(\varepsilon_F)$ of the B19′ M phase has also been found to be smaller than that of the B2 P phase.

If we suppose that the isovolume specific heat c_V can simply be broken down into the three contributions of phonon, $c_{V\,ph.}$, magnon, $c_{V\,mag.}$, and electron, $c_{V\,el.}$, as follows:

$$c_V = c_{V\,ph.} + c_{V\,mag.} + c_{V\,el.}, \tag{4}$$

then each component can be approximated as

$$c_{V\,mag.} = 0, \tag{5}$$

$$c_{P\,el.} \sim c_{V\,el.} = \gamma T, \tag{6}$$

and under the Debye theory,

$$c_{P\,ph.} \sim c_{V\,ph.} = 9R\left(\frac{T}{\Theta_D}\right)^3 \int_0^{\Theta_D/T} \frac{x^4 \exp(x)}{[\exp(x) - 1]^2} dx, \tag{7}$$

with the isobaric electronic and lattice specific heat ($c_{P\,el.}$ and $c_{P\,ph.}$). Equations 4–7 allow the estimation of temperature dependence of $c_P (= c_{P\,ph.} + c_{P\,el.})$ only using Θ_D and

Table 2 Debye temperature Θ_D and electronic specific heat coefficient γ of the prepared alloys

Ni content (at.%)		Θ_D (K)	$10^3 \cdot \gamma$ (J/mol K)
Nominal	Analytical		
50.00	49.98	356.5	2.527
50.50	50.55	346.8	2.498
51.00	50.92	326.4	2.852
51.20[a]	51.09	286.4	3.540
51.20[a]		288.4	3.420
51.60[a]	51.54	248.9	4.492
51.60[a]		252.1	4.483
51.80	51.75	242.4	4.573

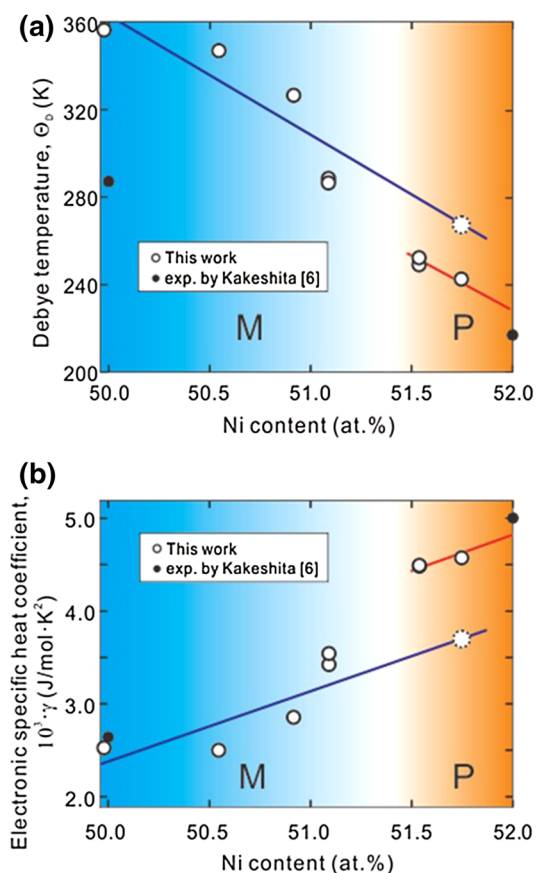[a] Two ingots of 51.2 and 51.6 Ni are prepared and measured

Fig. 5 Ni content dependences of **a** Debye temperature, Θ_D, and **b** electronic specific heat coefficient, γ [6], extracted from the data in Fig. 4

γ. Moreover, consequent c_P immediately leads to the derivations of entropy, S, and its constituting components of vibrational entropy, $S_{ph.}$, magnetic entropy, $S_{mag.}$, and electronic entropy, $S_{el.}$, by the following equations:

$$S = S_{ph.} + S_{mag.} + S_{el.}, \tag{8}$$

$$S_{mag.} = 0, \ S_{el.} \sim \gamma T, \ S_{ph.}(\Theta_D, T) = \int_0^T (c_{P\,ph.}/T)dT. \tag{9}$$

Using Eqs. 8–9, S and its constituents for the M and P phases in 51.75 Ni are calculated, where Θ_D and γ for the P phase are raw data of 242.4 K and 4.573 mJ/(mol K^2) and those for the M phase are estimated to be 270.8 K and 3.689 mJ/(mol K^2), respectively, by extrapolating these x dependences in the M phase region to 51.75 Ni (broken circles in Fig. 5a, b). The difference, $\Delta S_D(= S_D^P - S_D^M)$, which subtracts entropy of the M phase from that of the P phase, is represented by a blue line as a function of temperature in Fig. 3. It is seen that this Debye model-based ΔS_D curve is not in agreement with the experimental one.

To investigate the reason for such disagreement, c_P measurements up to 200 and 300 K were carried out for the 50.92 Ni M and 51.75 Ni P phases, resultant data ($c_{P\,exp.}$) being shown in Fig. 6a, b, respectively, together with the calculated $c_{P\,ph.}$, $c_{P\,el.}$, and $c_P(= c_{P\,ph.} + c_{P\,el.})$ using their own Θ_D and γ. Interestingly, a sharp contrast can be recognized between these specimens, that is, whereas the experimental and calculated c_P values in the M phase well accord with each other for all of the measured temperatures, those in the P phase remarkably differ in the temperature range 20–170 K (see the insets of Fig. 6a, b). This means that the Debye model with the experimental apparent Debye temperature fails to describe the temperature dependence of specific heat in the P phase. This may be attributed to the fact that the phonon softening exists in the Ni-rich Ti–Ni P phase [23–25]. In the same manner, experimentally obtained entropy, $S_{CP}(= \int_0^T (c_{P\,exp.}/T)dT)$, is presented in Fig. 6c, d. While showing a good agreement in the M phase of 50.92 Ni, the experimental and calculated S do not agree in the P phase of 51.75 Ni, except for the data below ∼20 K. Such deviation between the experimental and calculated S is observed only in the P phase of 51.75 Ni, directly resulting from the discrepancy in c_P as shown in Fig. 6b. Open circles in Fig. 3 are given as the difference $(\Delta S_{CP} = S_{CP}^P - S_{CP}^M)$ between the entropies obtained from the c_P measurements for 51.75 Ni (S_{CP}^P) and 50.92 Ni (S_{CP}^M). Even though obtained from the difference between two alloys with different compositions, the ΔS_{CP} gradually increases with increasing temperature, enabling a better fitting to the experimental plots than the Debye model-based ΔS_D.

All these results suggest that the drastic decrease of the experimental $\Delta S_{exp.}$ in the temperature region below about 280 K is apparently unusual, caused by the abnormal specific heat in the P phase rather than in the M phase. It has been reported that an incommensurate–commensurate (IC-C) transition, referred to as the resultant precursor state of the above-mentioned lattice softening [27, 28], occurs at the temperature around which ER starts to increase. Another possibility is that it occurs by the strain glass phenomenon. In any case, what relatively stabilizes the P phase may occur in the temperature region below around 300 K.

Composition–Temperature Phase Diagram

The phase equilibrium condition between an external field, such as pressure, magnetic field, or uniaxial stress, and temperature is usually expressed by the CC equation. This can apparently be expanded to the relation between composition and temperature such as x_0–T phase diagram,
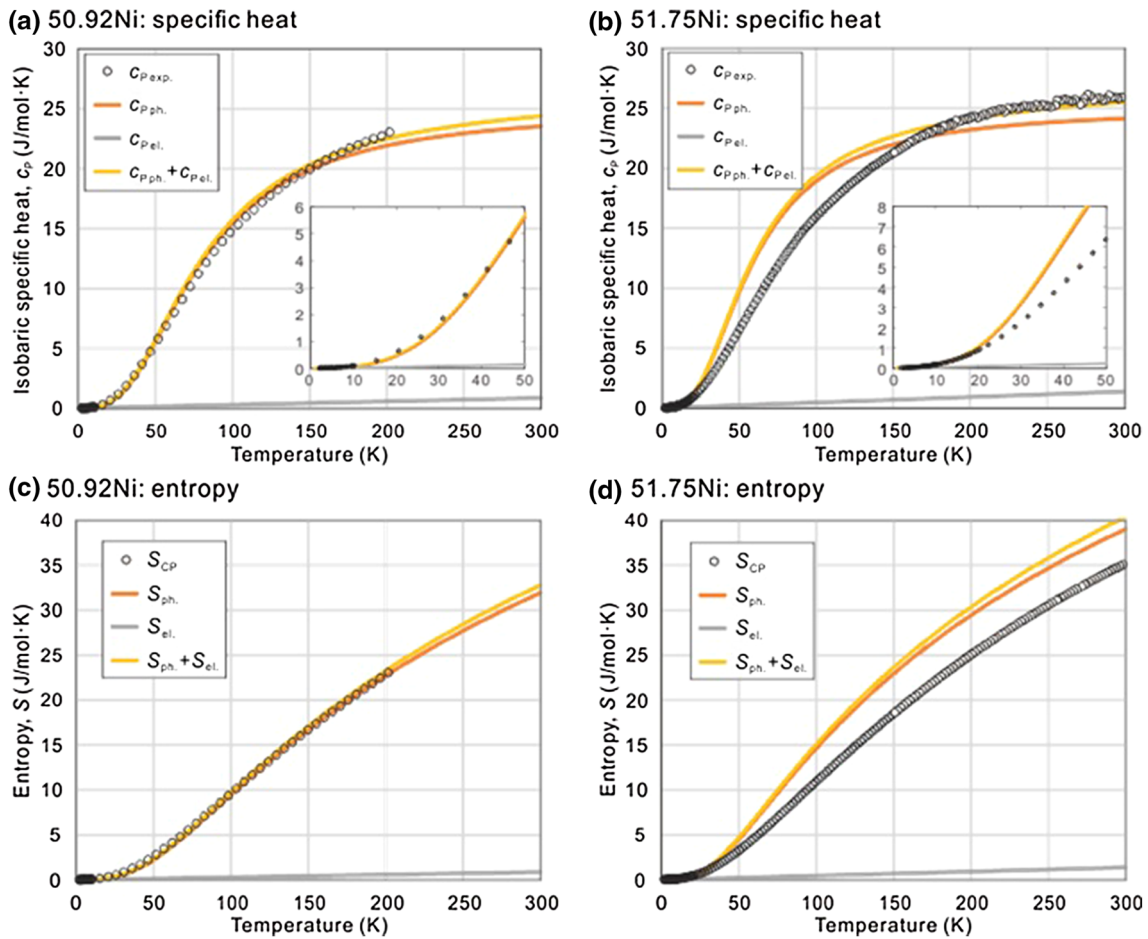
Fig. 6 Temperature dependences of $c_{P\,exp.}$ (experimentally obtained isobaric specific heat), $c_{P\,ph.}$, and $c_{P\,el.}$ (phonon and electron components of calculated isobaric specific heat, respectively) and their sum for **a** M (50.92 Ni) and **b** P (51.75 Ni) phases. Temperature

dependences of $S_{exp.}$ (experimentally obtained entropy), $S_{ph.}$, and $S_{el.}$ (phonon and electron components of calculated entropy, respectively) and their sum for **a** M (50.92 Ni) and **b** P (51.75 Ni) phases

where x_0 is the equilibrium composition at which the Gibbs energy of the P phase is equal to that of the M phase, in the present case.

When considering Gibbs energies of the P and M phases in the Ti–Ni binary system under equilibrium,

$$G^M = G^P.$$

The differentiation is

$$dG^M = dG^P.$$

Since $dG^i = -S^i dT + \mu_{Ti}^i dx_0^{Ti} + \mu_{Ni}^i dx_0^{Ni}$ for the i phase in a fixed pressure,

$$-S^M dT + \mu_{Ti}^M dx_0^{Ti} + \mu_{Ni}^M dx_0^{Ni} = -S^P dT + \mu_{Ti}^P dx_0^{Ti} + \mu_{Ni}^P dx_0^{Ni}$$

$$S^M dT + \left(\mu_{Ti}^M - \mu_{Ni}^M\right) dx_0^{Ni} = S^P dT + \left(\mu_{Ti}^P - \mu_{Ni}^P\right) dx_0^{Ni}.$$

Then, the CC relation for x_0–T system is given by

$$\frac{dT}{dx_0^{Ni}} = -\frac{\left(\mu_{Ti}^P - \mu_{Ni}^P\right) - \left(\mu_{Ti}^M - \mu_{Ni}^M\right)}{S^P - S^M} = -\frac{\Delta\mu_{Ti} - \Delta\mu_{Ni}}{\Delta S}, \tag{10}$$

where S^i is entropy, μ_{Ti}^i and μ_{Ni}^i are chemical potentials of Ti and Ni of the i phase, respectively, and $x_0^{Ni} (= 1 - x_0^{Ti})$ is the equilibrium Ni fraction of alloy. $\Delta\mu_{Ti}$ and $\Delta\mu_{Ni}$ are the differences in the chemical potentials of the constituting elements Ti and Ni between the P and M phases, and $(\Delta\mu_{Ti} - \Delta\mu_{Ni}) = -\left(\partial G^P/\partial x_0^{Ni} - \partial G^M/\partial x_0^{Ni}\right)$. This equation manifests $dT/dx_0^{Ni} \to -\infty$ as $T \to 0$, since ΔS usually converges to zero as T approaches 0 K. In comparison with Eq. 1, Eq. 10 can be modified as

$$\frac{dT}{dx_0^{Ni}} = \frac{dT}{d\sigma_0} \cdot \frac{\Delta\mu_{Ti} - \Delta\mu_{Ni}}{\varepsilon \cdot V_m}. \tag{11}$$

This means that the temperature dependence of x_0 should be similar to that of σ_0, when the temperature and

composition dependences of $(\Delta\mu_{Ti} - \Delta\mu_{Ni})$ and $\varepsilon \cdot V_m$ are negligible.

In order to convert the σ_0–T relation to the x_0–T relation using Eq. 11, the numerical values of ε, V_m, and $(\Delta\mu_{Ti} - \Delta\mu_{Ni})$ need to be estimated. The ε and V_m can be assumed to be simply constant: $\varepsilon = 0.044$ and $V_m = 8.25 \times 10^{-6}$ m^3/mol, independent of temperature and alloy composition. The numerical values of $(\Delta\mu_{Ti} - \Delta\mu_{Ni})$ were evaluated by Eq. 10 from the ΔS determined for the 49.98 and 50.92 Ni alloys (see Table 1) and the slope of x–T_0 curve shown in Fig. 2. The $(\Delta\mu_{Ti} - \Delta\mu_{Ni})$ evaluated for 49.98 and 50.92 Ni are about 44 and 48 kJ/mol, respectively, being roughly independent of alloy composition. Under a simple condition that all the values of ε, V_m, and $(\Delta\mu_{Ti} - \Delta\mu_{Ni})$ are constant, the conversion between stress- and concentration-field can be given by

$$\Delta x_0^{Ni} \approx \frac{\varepsilon \cdot V_m}{\Delta\mu_{Ti} - \Delta\mu_{Ni}} \cdot \Delta\sigma_0 = C\Delta\sigma_0. \tag{12}$$

When $(\Delta\mu_{Ti} - \Delta\mu_{Ni}) = 48$ kJ/mol for 50.92 Ni is used, the constant, C, becomes 7.6×10^{-9} m^3/kJ ($= 7.6 \times 10^{-6}$ MPa^{-1}), in which $\Delta\sigma_0 = 1000$ MPa is equivalent to $\Delta x_0^{Ni} = 0.0076$ (=0.76 at.%). It is apparent that Eq. 12 is available for conversion not only of $\sigma_0 \rightarrow x_0$, but also of $\sigma_{Ms} \rightarrow x_{Ms}$ and $\sigma_{Af} \rightarrow x_{Af}$, because it simply converts mechanical energy to chemical energy. Figure 7a exhibits x_0, x_{Ms}, and x_{Af} curves obtained from σ_0, σ_{Ms}, and σ_{Af} curves in Fig. 7b, respectively, where the original point of the composition curves is set at 51.67 Ni, but not at 51.75 Ni. Such a shift of the original point was performed in accordance with the following experimental data on reverse transformation stress. In the case of the σ_{Af} curve for 51.75 Ni in Fig. 7b, $\sigma_{Af} = 0$ is obtained at about 40 K, which may correspond to T_{Af} for this composition. It is known that T_{Af} estimated from SIT is not always coincident with the thermal transformation temperature. In the present alloy, it has been reported that the thermal transformation temperatures are comparable to those evaluated from the critical stress of SIT [4]. The other T_{Af} values evaluated by the same method for 51.30 and 51.59 specimens [29] are plotted by filled circles in Fig. 7(a). The original point of the x–T curves converted from the σ–T ones was determined by fitting to these T_{Af} data.

As shown in Fig. 7a, the x_0, x_{Ms}, and x_{Af} curves proposed at temperatures below 180 K almost perfectly connect, respectively, with T_0, T_{Ms}, and T_{Af} curves determined at higher temperatures. Moreover, the x_{Ms} (namely, T_{Ms}) curve has an inverted C-shape with a maximum at about 120 K around 51.22 Ni, which means that the T_{Ms} suddenly disappears at this composition and that MT does not occur at temperatures below around 120 K. Thus, the reason why the T_{Ms} suddenly disappears at around 51.4 at.% Ni [3] is explained by the temperature dependence of x_{Ms} with an inverted C-shape,
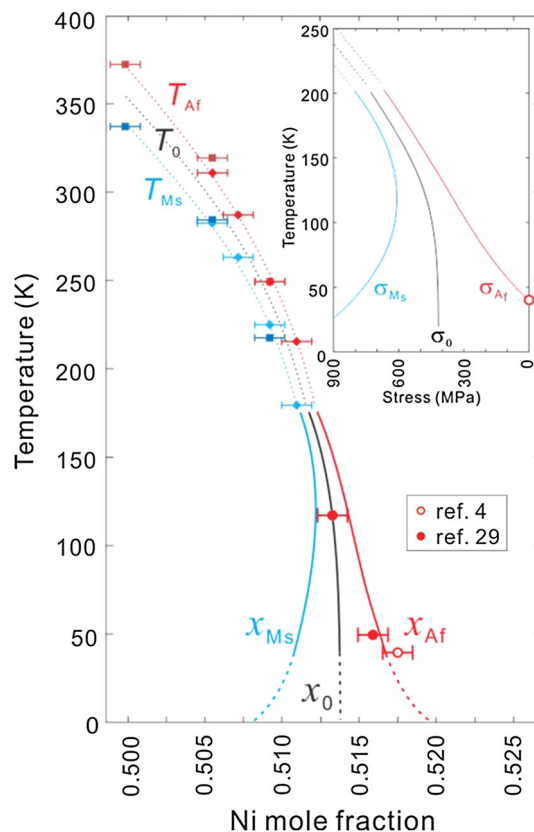

Fig. 7 a Composition–temperature phase diagram in an Ni-rich Ti–Ni portion. In **a**, transformation temperatures, T_0, T_{Ms}, and T_{Af}, above 180 K are experimentally determined (broken lines) and critical compositions, x_0, x_{Ms}, and x_{Af}, below 180 K are speculated using CC equations of Eqs. 10–12 (solid lines). Closed and open red circles are T_{Af} (118 K in 51.30 Ni, 50 K in 51.59 Ni [29], and 40 K in 51.75 Ni [4]), which correspond to a temperature giving $\sigma_{Af} = 0$ in the stress–temperature phase diagram as shown in **b**. **b** Stress–temperature phase diagram in 51.75 Ni [4]

which is obviously brought about by the drastic increase of "composition hysteresis" reflecting stress hysteresis at low temperatures. Such a dramatic increase of hysteresis is explained by the existence of a thermal activation term in friction against migration of the P/M phase interface and analyzed by a phenomenological theory in Ref. [30, 31].

Conclusions

For some Ni-rich Ti–Ni alloys, B2/B19′ martensitic transformation temperatures, transformation entropy change, and specific heat were precisely determined and the following results were obtained:

1. With increasing Ni composition from 49.98 Ni, while gradually decreasing in the beginning, martensitic transformation temperatures acceleratedly decline toward the high-Ni content region of ∼51 % and are not detected in compositions over 51.23 %.

2. Although the values of entropy change evaluated from DSC measurement for 49.98–50.75 Ni are roughly the same, those for 50.92 Ni are almost half of those in the lower Ni alloys. The entropy change plotted to T_0 temperature shows an S-shaped curve, which starts to drastically decrease at about 300 K.

3. The entropy change estimated from direct measurements of specific heat for 51.75 Ni (B2) and 50.92 Ni (B19$'$) is more consistent with the experimental data, rather than the calculated curve based on the Debye model for vibration specific heat, which is attributed to the lattice instability inherent in the parent phase.

4. The Clausius–Clapeyron equation for the x–T system was proposed, and a previously reported σ–T diagram was converted to an x–T diagram. The derived x–T phase diagram below 180 K is almost completely compatible with that above 180 K experimentally determined. Moreover, the reason for the sudden disappearance of T_{Ms} around 51.4 Ni was successfully explained by the inverted-C-shaped behavior of x_{Ms} (T_{Ms}) line converted from σ_{Ms}.

References

1. Zhang Z, Wang Y, Wang D, Zhou Y, Otsuka K, Ren X (2010) Phase diagram of Ti$_{50-x}$Ni$_{50+x}$: crossover from martensite to strain glass. Phys Rev B 81:224102

2. Sarkar S, Ren X, Otsuka K (2005) Evidence for strain glass in the ferroelastic-martensite system Ti$_{50-x}$Ni$_{50+x}$. Phys Rev Lett 95:205702

3. Ren X, Wang Y, Zhou Y, Zhang Z, Wang D, Fan G, Otsuka K, Suzuki T, Ji Y, Zhang J, Tian Y, Hou S, Ding X (2010) Strain glass in ferroelastic systems: premartensitic tweed versus strain glass. Philos Mag 90(1–4):141–157

4. Niitsu K, Omori T, Kainuma R (2013) Stress-induced transformation behaviors at low temperatures in Ti-51.8Ni (at.%) shape memory alloy. Appl Phys Lett 102:231915

5. Tong HC, Wayman CM (1974) Characteristic temperatures and other properties of thermoelastic martensites. Acta Metall 22(7):887–896

6. Kakeshita T, Fukuda T, Tetsukawa H, Saburi T, Kindo K, Takeuchi T, Honda M, Endo S, Taniguchi T, Miyako Y (1998) Negative temperature coefficient of electrical resistivity in B2-type Ti–Ni alloys. Jpn J Appl Phys 37:2535–2539

7. Miyazaki S, Otsuka K (1986) Deformation and transition behavior associated with the R-phase in Ti-Ni alloys. Metall Trans A 17(1):53–63

8. Honma T, Takei H (1975) Effect of heat treatment on the martensitic transformation in Ti-Ni alloys. J Jpn Inst Met 39:175–182 **(in Japanese)**

9. Choi MS, Fukuda T, Kakeshita T (2005) Anomalies in resistivity, magnetic susceptibility and specific heat in iron-doped Ti–Ni shape memory alloys. Scr Mater 53(7):869–873

10. Hanlon JE, Butler SR, Wasilewski RJ (1967) Effect of martensitic transformation on the electrical and magnetic properties of NiTi. Trans AIME 239:1323–1327

11. Kornilov II, Kachur Ye V, Belousov OK (1971) Diffraction transformation in the compound TiNi. Fiz Met Metalloved 32(2):420–421

12. Melton KN, Mercier O (1981) The mechanical properties of NiTi-based shape memory alloys. Acta Metall 29(2):393–398

13. Miyazaki S, Otsuka K, Suzuki Y (1981) Transformation pseudoelasticity and deformation behavior in a Ti-50.6at%Ni alloy. Scr Mater 15:287–292

14. Nishida M, Wayman CM, Honma T (1986) Precipitation processes in near-equiatomic TiNi shape memory alloys. Metall Trans A 17(9):1505–1515

15. Wasilewski RJ, Butler SR, Hanlon JE (1967) On the martensitic transformation in TiNi. Met Sci 1(1):104–110

16. Wasilewski RJ, Butler SR, Hanlon JE, Worden D (1971) Homogeneity range and the martensitic transformation in TiNi. Metall Trans 2(1):229–238

17. Tang W (1997) Thermodynamic study of the low-temperature phase B19$'$ and the martensitic transformation in near-equiatomic Ti-Ni shape memory alloys. Metall Mater Trans A 28(3):537–544

18. Tang W, Sandström R, Wei ZG, Miyazaki S (2000) Experimental investigation and thermodynamic calculation of the Ti-Ni-Cu shape memory alloys. Metall Mater Trans A 31(10):2423–2430

19. Bogdanoff PD, Fultz B (2001) The role of phonons in the thermodynamics of the martensitic transformation in NiTi. Philos Mag B 81(3):299–311

20. Smith JF, Jiang Q, Lück R, Predel B (1991) C_p and fractal phase transformation in the shape memory alloy Ni-52Ti. Mater Sci Eng 149A:111–120

21. Ono N, Satoh A, Ohta H (1989) A discussion on the mechanical properties of shape memory alloys based on a polycrystal model. Mater Trans JIM 30(10):756–764

22. Gopal ESR (1966) Specific heats at low temperatures. Plenum Press, New York

23. Moine P, Allain J, Renker B (1984) Observation of a soft-phonon mode and a pre-martensitic phase in the intermetallic compound Ti$_{50}$Ni$_{47}$Fe$_3$ studied by inelastic neutron scattering. J Phys F 14(11):2517

24. Tietze H, Mullner M, Renker B (1984) Dynamical properties of premartensitic NiTi. J Phys C 17(21):L529

25. Zhao GL, Harmon BN (1993) Electron-phonon interactions and the phonon anomaly in β-phase NiTi. Phys Rev B 48:2031

26. Fukuda T, Kakeshita T, Houjoh H, Shiraishi S, Saburi T (1999) Electronic structure and stability of intermetallic compounds in the Ti–Ni System. Mater Sci Eng A 273–275:166–169

27. Hwang CM, Meichle M, Salamon MB, Wayman CM (1983) Transformation behaviour of a Ti$_{50}$Ni$_{47}$Fe$_3$ alloy I. Premartensitic phenomena and the incommensurate phase. Philos Mag A 47(1):9–30

28. Murakami Y, Shibuya H, Shindo D (2001) Precursor effects of martensitic transformations in Ti-based alloys studied by electron microscopy with energy filtering. J Microsc 203:22

29. Niitsu K (2014) Superelastic properties at cryogenic temperatures in Ti-Ni, Ni-Co-Mn-In and Cu-Al-Mn shape memory alloys. Ph.D. Thesis, Tohoku University, Japan

30. Niitsu K, Xu X, Umetsu RY, Kainuma R (2013) Stress-induced transformations at low temperatures in a Ni$_{45}$Co$_5$Mn$_{36}$In$_{14}$ metamagnetic shape memory alloy. Appl Phys Lett 103:242406

31. Umetsu RY, Endo K, Kondo A, Kindo K, Ito W, Xu X, Kanomata T, Kainuma R (2013) Magnetoresistance and transformation hysteresis in the Ni$_{50}$Mn$_{34.4}$In$_{15.6}$ metamagnetic shape memory alloy. Mater Trans 54(3):291–296